green color persisted for more than 20 min. Ethylene oxide was condensed to a liquid (0.21 mL) and added to the reaction mixture. The flask was sealed and heated at 45 °C for 8 h. After cooling to room temperature, the THF was removed by rotatory evaporation. Filtration through a plug of silica gel removed DMSO and naphthalene by-products (**7**: 0.61 g, 98 % yield). ^{1}H NMR (500 MHz, CD_2Cl_2): $\delta = 6.95$ (br m, 73 H), 3.57 (br m, 72 H), 3.17 (br m, 2 H), 2.24 (br m, 8 H), 1.05 (br m, 13 H), 0.85 (m, 3 H); GPC (254 nm, THF): PDI = 1.13, $M_n = 1489$.

1: ^{1}H NMR (500 MHz, CD_2Cl_2): $\delta = 6.95$ (br m, 120 H), 3.57 (br m, 80 H), 2.24 (br m, 8 H), 1.05 (br m, 13 H), 0.85 (m, 3 H); GPC (254 nm, THF): PDI = 1.15, $M_n = 2277$.

Received: August 26, 1999 [Z13928]

[1] J. M. Lehn, *Supramolecular Chemistry*, VCH, New York, **1995**.
[2] *Comprehensive Supramolecular Chemistry*, *Vol. 11* (Eds.: J. L. Atwood, J. E. D. Davies, D. D. MacNicol, F. Vögtle), Pergamon, New York, **1996**.
[3] S. I. Stupp, V. LeBonheur, K. Walker, L. S. Li, K. Huggins, M. Keser, A. Amstutz, *Science* **1997**, *276*, 384 – 389.
[4] E. R. Zubarev, M. U. Pralle, L. M. Li, S. I. Stupp, *Science* **1999**, *283*, 523 – 526.
[5] M. U. Pralle, C. M. Whitaker, P. V. Braun, S. I. Stupp, unpublished results.
[6] G. N. Tew, L. M. Li, S. I. Stupp, *J. Am. Chem. Soc.* **1998**, *120*, 5601 – 5602.
[7] G. N. Tew, M. U. Pralle, S. I. Stupp, *J. Am. Chem. Soc.* **1999**, in press.
[8] *Polymers for Light Wave and Integrated Optics* (Ed.: L. A. Hornak), Marcel Dekker, New York, **1992**.
[9] M. Morton, *Anionic Polymerization: Principles and Practice*, Academic Press, New York, **1983**.
[10] J. Lindsey, *Tetrahedron* **1984**, *40*, 1433 – 1456.
[11] J. F. Hartwig, *Angew. Chem.* **1998**, *110*, 2154 – 2177; *Angew. Chem. Int. Ed.* **1998**, *37*, 2047 – 2067.
[12] J. P. Wolfe, S. Wagaw, S. L. Buchwald, *J. Am. Chem. Soc.* **1996**, *118*, 7215 – 7216.
[13] M. Kosugi, M. Kameyama, T. Magita, *Chem. Lett.* **1983**, 927 – 930.
[14] S. Thayumanavan, S. Barlow, S. R. Marder, *Chem. Mater.* **1997**, *9*, 3231 – 3235.
[15] G. N. Tew, L. M. Li, M. U. Pralle, S. I. Stupp, *Abstr. Pap. MRS* (Boston, MA) **1997**, p. J3.35.
[16] W. J. Feast, R. J. Peace, I. A. Sage, E. L. Wood, *Polym. Bull.* **1999**, *42*, 167 – 174.
[17] R. G. Compton, M. E. Laing, A. Ledwith, I. Abu-Abdoun, *J. Appl. Electrochem.* **1988**, *18*, 431 – 440.
[18] M. A. Hillmyer, F. S. Bates, *Macromolecules* **1996**, *29*, 6194 – 7002.
[19] T. Granier, E. L. Thomas, D. R. Gagnon, F. E. Karasz, R. W. Lenz, *J. Polym. Sci. B* **1986**, *24*, 2793 – 2804.
[20] The fact that the TPA and PV chromophores both have absorbance at 302 nm makes the interpretation of energy transfer more difficult. To determine if indeed energy transfer is occurring several experiments were performed. The absorption and emission spectra were measured in six different dielectric solvents to rule out electron transfer; the solvents, in order of decreasing dielectric constant, were acetonitrile, tetrahydrofuran, chloroform, diethyl ether, benzene, and cyclohexane. There was no observable shift in λ_{max} for absorption or emission. A series of different concentrations was investigated with UV/Vis spectroscopy to ensure no molecular aggregation was occurring in solution. The concentration was varied from optical density of 0.1 to 1.1 absorbance units. Finally, quantum efficiencies (ϕ) were determined to be $\phi = 0.07$ for **6** and $\phi = 0.04$ for **1**.
[21] D. M. Watkins, M. A. Fox, *J. Am. Chem. Soc.* **1996**, *118*, 4344 – 4353.
[22] S. E. Webber, *Chem. Rev.* **1990**, *90*, 1469 – 1482.

Kinetic Footprinting of an RNA-Folding Pathway Using Peroxynitrous Acid**

Steven G. Chaulk and Andrew M. MacMillan*

Complex RNA molecules are at the heart of a number of fundamental biological processes, including translation, tRNA maturation, and RNA splicing.[1] The unique three-dimensional structures adopted by these molecules determine their activity and in some cases, such as the assembly of the spliceosome, a dynamic series of rearrangements of the RNA structure is required to assemble an active catalytic complex. Considerable progress has been made, using phylogenetic, X-ray, NMR, and chemical probing techniques, towards understanding the two- and three-dimensional structures adopted by large RNAs.[2–8] The mechanisms and pathways by which large RNAs fold into these structures are obviously of interest, and there is a need for novel approaches to study these processes.

One of the most powerful techniques for probing nucleic acid structure is chemical footprinting. Diffusable hydroxyl radicals produced from Fe-ethylenediaminetetraacetate (EDTA) or Cu-phenanthroline complexes effect cleavage of the phosphodiester backbone of both DNA and RNA; cleavage of radio-labeled molecules can be easily analyzed on high-resolution polyacrylamide gels.[9, 10] Protection against such cleavage through binding of a protein or formation of a higher order structure is detected as an area of reduced cleavage or footprint. These commonly used footprinting techniques may be regarded as *thermodynamic* since the radicals are typically generated over a 10 – 60 minute time period and thus are useful for examining a system at equilibrium. Elegant *kinetic* footprinting studies were performed by Chance, Brenowitz, Woodson, and co-workers to elucidate the folding pathway of the Group I ribozyme—radicals were produced on a 50 – 100 ms timescale by synchrotron X-ray irradiation of folding reactions and allowed the visualization of discrete intermediates on the folding pathway.[11] Our interest in the dynamics of RNA structure has prompted us to explore the application of other readily available chemical footprinting reagents to kinetic studies of RNA folding. Here we describe the first use of such a reagent, peroxynitrous acid, as a tool for examining the folding pathway of a complex RNA: the *Tetrahymena* ribozyme.

Peroxynitrous acid (HOONO) is unstable in aqueous solution, undergoing homolytic cleavage to generate hydroxyl radical and nitrogen dioxide,[12, 13] and has been employed in

[*] Prof. A. M. MacMillan, S. G. Chaulk
Department of Chemistry
University of Toronto
Toronto, ON, M5S-3H6 (Canada)
Fax: (+1) 416-978-8603
E-mail: amacmill@chem.utoronto.ca

[**] A.M.M. acknowledges support from the Natural Sciences and Engineering Research Council of Canada. The authors are grateful to Vernon Anderson for calling their attention to peroxynitrous acid as a footprinting reagent. We thank Martha Rook and Jamie Williamson for providing plasmid pT7L-21 and we are grateful to Vanita Sood and Rick Collins for helpful discussions.

  0570-0833/00/3903-0521 $ 17.50+.50/0

footprinting studies of tRNA and of a *lac* repressor/DNA complex.[14, 15] The reagent is conveniently stored as the stable potassium salt in basic solution, and radical formation may be initiated by dilution into a neutral buffered reaction [Eq. (1)].

$$KOONO \xrightarrow{H^+} HOONO \rightarrow HO^{\cdot} + NO_2^{\cdot} \quad (1)$$

The half-life of the decomposition process is between one and two seconds at neutral pH;[16] the observation that many RNA folding events occur on a timescale of minutes[17] immediately suggests the potential of HOONO as a kinetic footprinting reagent in such systems.

We chose the L-21 *Tetrahymena* ribozyme, a 385 nucleotide sequence-specific endoribonuclease derived from a self-splicing Group I intron, as a model system for our studies because it has been exceptionally well characterized biochemically and because the structures of several large fragments have been determined by X-ray crystallography.[3, 4] Phylogenetic comparisons[2] were originally used to predict a number of conserved paired regions (P) and provided a two-dimensional map of the ribozyme structure (Figure 1a)—the folding of the RNA into its active three-dimensional structure is a magnesium-dependent process which produces a compact structure of tightly packed helical regions.[3, 4] Equilibrium footprinting of the *Tetrahymena* ribozyme with Fe-EDTA showed a strong, magnesium-dependent protection of the P3 and P4 regions (highlighted in Figure 1a).[9]

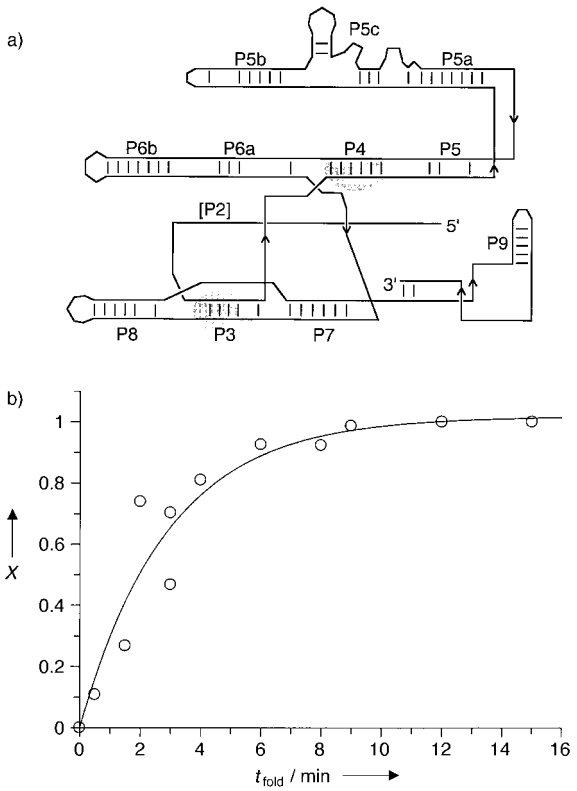

Figure 1. a) Schematic representation of the secondary structure of the *Tetrahymena* L-21 *Sca*I ribozyme showing base-paired (P) regions. The P3 and P4 regions, which are strongly protected from radical-induced cleavage in the folded RNA molecule,[9] are shaded; b) folding of the ribozyme, assayed through analysis of endoribonuclease activity following addition of Mg^{2+}. *X* represents the fraction of RNA cleaved at a particular folding time, normalized to the final observed cleavage. Cleavage reactions were carried out with excess ribozyme for 50 s. The first-order rate constant for the overall folding process k_{fold} is $\sim 0.4\ min^{-1}$.

We synthesized the ribozyme by T7 run-off transcription from the plasmid pT7L-21 and assayed it for activity in the cleavage of a ^{32}P-labeled 11 nucleotide RNA substrate.[17] By using this activity as an assay for magnesium-dependent folding of the ribozyme[17] we were able to observe a folding process taking place over several minutes with an observed rate k_{fold} of $0.4\ min^{-1}$ (Figure 1b).

We carried out the kinetic footprinting studies by the addition of freshly prepared potassium peroxynitrite to folding reactions containing ^{32}P-end-labeled RNA at various time points following the addition of magnesium chloride. Reactions were desalted by precipitation and analyzed by denaturing gel electrophoresis (Figure 2a). Control cleavages with RNase T1 were carried out to create a G ladder and thus allow mapping of cleavage sites to specific regions of the ribozyme sequence. It is apparent that the addition of Mg^{2+} results in significant protection of portions of the ribozyme

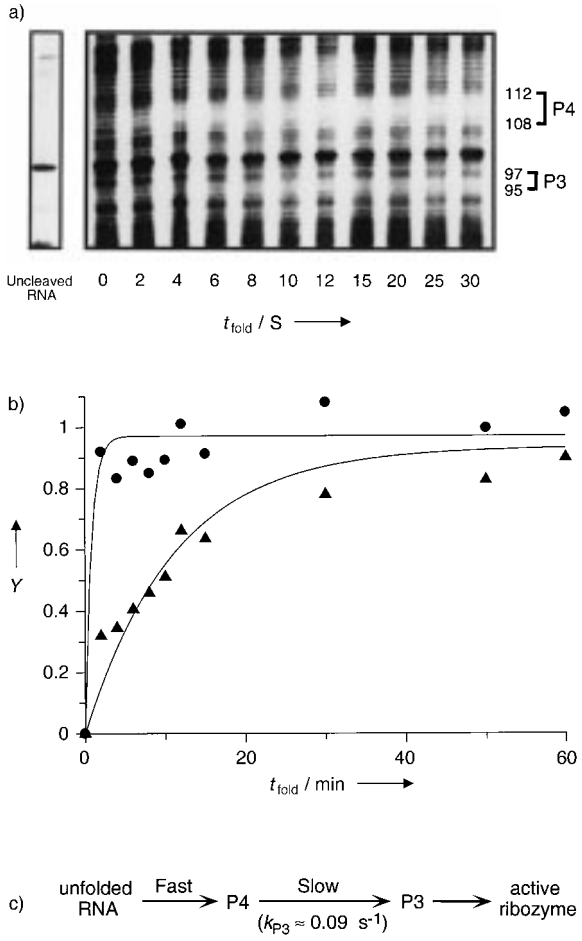

Figure 2. Peroxynitrous acid footprinting of the ribozyme during folding. a) Lower portion of a gel showing cleavage of the ribozyme at indicated times following addition of Mg^{2+}. The position of cleavage is shown by reference to paired regions described in Figure 1a; b) relative protection of the P3 (▲) and P4 (●) regions of the ribozyme as a function of folding time. *Y* represents the fraction of RNA protected from cleavage, relative to unfolded RNA, at a given folding time; c) partial hierarchy of the folding pathway of the *Tetrahymena* ribozyme.

  0570-0833/00/3903-0522 $ 17.50+.50/0

from radical-induced cleavage. In order to assess the time and domain dependence of such cleavage, we quantified cleavages over specific regions and plotted these as a fraction of relative protection versus time (Figure 2b). This analysis suggests that individual domains of the ribozyme assemble at different rates (Figure 2c) and is consistent with the results of both synchrotron X-ray footprinting[11] and an oligonucleotide hybridization/cleavage assay,[17] two other methods that have been used to analyze the folding pathway of the *Tetrahymena* ribozyme. The P4-P6 region is protected very quickly during the folding process and has been proposed as a scaffold around which other folding events take place.[18] Assembly of the P3 helix at the core of the catalytic domain is a late-occurring event and may be reflective of kinetic traps along the folding pathway.[19]

The formation of the P4 helix clearly occurs too fast to be measured with the peroxynitrous acid reagent—analysis of events such as these requires the more rapid radical generation available through synchrotron irradiation. However, formation of the P3 helix is significantly slower. This event takes place with a first-order rate constant (k_{P3} 0.09 s^{-1}); the half-time for protection is roughly eight seconds. A comparison with the overall rate of folding (Figure 1b) indicates that P3 formation is not the rate determining step—we are carrying out additional investigations, including an analysis of the rates of folding of other regions of the ribozyme.

Our results with the *Tetrahymena* system validate the use of peroxynitrous acid as a kinetic footprinting tool; this easily used methodology should prove valuable in the elucidation of many relatively slow RNA folding pathways and the examination of RNA dynamics in complex systems.

Experimental Section

Potassium peroxynitrite synthesis: HCl (0.5 M, 5 mL) was added to a stirred ice-cooled aqueous solution (10 mL) containing $NaNO_2$ (0.6 M, 0.41 g) and H_2O_2 (3%). A solution (5 mL) containing diethylenetriaminepentaacetic acid (400 μM, 3.3 mg) and KOH (1.6 M) was added immediately afterwards. The resulting mixture was stirred for 5 minutes then MnO_2 (100 mg) was added and stirring continued for 20 minutes. Excess MnO_2 was removed by gravity filtration (performed at 4 °C). Typical yields of potassium peroxynitrite were 80–130 mM measured by UV absorbance at 302 nm (ε = 1670 $M^{-1}cm^{-1}$). Even a slight delay in the addition of the KOH/diethylenetriaminepentaacetic acid solution resulted in significantly lower yields of potassium peroxynitrite. The potassium peroxynitrite solution was stored at −78 °C with no decrease in concentration after 10 weeks.

Peroxynitrous acid footprinting: L-21 Group I ribozyme folding was initiated by the addition of $MgCl_2$ (final concentration 10 mM) to a solution (final volume 20 μL) containing final concentrations of NaCl (80 mM), NaH_2PO_4/Na_2HPO_4 (50 mM, pH 7), 5′-end labeled ribozyme (50 nM, 3×10^6 cpm) at 22 °C. Footprinting was then effected by the addition of potassium peroxynitrite (1 μL, 130 mM) at the indicated times (see Figure 2). Footprinting reactions were allowed to proceed for 20 seconds before freezing on dry ice, followed by ethanol precipitation. Reactions (1×10^6 cpm) were then subjected to denaturing polyacrylamide gel electrophoresis (PAGE, 6%, 19:1) for 2.3 hours at 85 W. Dried gels were exposed to a molecular dynamics phosphor screen, which was then scanned on a Molecular Dynamics Storm 860 Phosphorimager. To calculate the fractional peroxynitrous acid protection (footprint), the background intensity (ImageQuant 5.0) was first subtracted and a correction for differences in lane loading was applied. The intensity of a region at a given time was divided by the intensity of the same region at time zero. The resulting fractional intensities were normalized from 0 to 1. Plots of normalized fractional protection versus folding time were fitted to a first-order exponential (GraFit 3.00) using data averaged from five separate experiments.

Received: July 26, 1999 [Z13782]

[1] See *The RNA world*, 2nd ed. (Eds.: R. F. Gesteland, T. R. Cech, J. F. Atkins), Cold Spring Harbor Laboratory, Cold Spring Harbor, **1999**.
[2] F. Michel, E. Westhof, *J. Mol. Biol.* **1990**, *216*, 585–610.
[3] J. H. Cate, A. R. Gooding, E. R. Podell, K. Zhou, B. L. Golden, C. E. Kundrot, T. R. Cech, J. A. Doudna, *Science* **1996**, *273*, 1678–1685.
[4] B. L. Golden, A. R. Gooding, E. R. Podell, T. R. Cech, *Science* **1998**, *282*, 259–264.
[5] W. G. Scott, *Curr. Opin. Struct. Biol.* **1998**, *8*, 720–726.
[6] M. Wu, I. Tinoco, Jr., *Proc. Natl. Acad. Sci. USA* **1998**, *95*, 11555–11560.
[7] A. A. Szewczak, L. Ortoleva-Donnelly, S. P. Ryder, E. Moncoeur, S. A. Strobel, *Nat. Struct. Biol.* **1998**, *5*, 1037–1042.
[8] R. T. Batey, R. P. Rambo, J. A. Doudna, *Angew. Chem.* **1999**, *111*, 2472–2491; *Angew. Chem. Int. Ed.* **1999**, *38*, 2326–2343.
[9] J. A. Latham, T. R. Cech, *Science* **1989**, *245*, 276–282.
[10] C.-H. B. Chen, D. S. Sigman, *J. Am. Chem. Soc.* **1988**, *110*, 6570–6572.
[11] a) B. Sclavi, S. A. Woodson, M. Sullivan, M. R. Chance, M. Brenowitz, *J. Mol. Biol.* **1997**, *266*, 144–159; b) B. Sclavi, M. Sullivan, M. R. Chance, M. Brenowitz, S. A. Woodson, *Science* **1998**, *279*, 1940–1943.
[12] C. E. Richeson, P. Mulder, V. W. Bowry, K. U. Ingold, *J. Am. Chem. Soc.* **1998**, *120*, 7211–7219.
[13] P. A. King, V. E. Anderson, J. O. Edwards, G. Gustafson, R. C. Plumb, J. W. Suggs, *J. Am. Chem. Soc.* **1992**, *114*, 5430–5432.
[14] P. A. King, E. Jamison, D. Strahs, V. E. Anderson, M. Brenowitz, *Nucleic Acids Res.* **1993**, *21*, 2473–2478.
[15] M. Götte, R. Marquet, C. Isel, V. E. Anderson, G. Keith, H. J. Gross, B. Ehresmann, H. Heumann, *FEBS Lett.* **1996**, *390*, 226–228.
[16] J. S. Beckman, T. W. Beckman, J. Chen, P. A. Marshall, B. A. Freeman, *Proc. Natl. Acad. Sci. USA* **1990**, *87*, 1620–1624.
[17] P. P. Zarrinkar, J. R. Williamson, *Science* **1994**, *265*, 918–924.
[18] E. A. Doherty, J. A. Doudna, *Biochemistry* **1997**, *36*, 3159–3169.
[19] M. S. Rook, D. K. Treiber, J. R. Williamson, *J. Mol. Biol.* **1998**, *281*, 609–620.

Solvation of the Carbonyl Compound as a Predominant Factor in the Diastereofacial Selectivity of Nucleophilic Addition**

Gianfranco Cainelli,* Paola Galletti, Daria Giacomini,* and Paolo Orioli

Discussions of factors controlling stereoselectivity commonly focus on steric and/or electronic features of the catalyst and/or the substrate.[1] However, selectivity is a kinetic

[*] G. Cainelli, D. Giacomini, P. Galletti, P. Orioli
Dipartimento di Chimica "G. Ciamician"
Via Selmi 2, 40126 Bologna (Italy)
Fax: (+390) 51-209-9456
E-mail: cainelli@ciam.unibo.it, giacomin@ciam.unibo.it

[**] This work was supported by MURST and the University of Bologna (Fund for Selected Topics). We thank Andrea Garelli for assistance with the NMR spectroscopy.